PERGAMON

Journal of Structural Geology 24 (2002) 1521–1535

JOURNAL OF STRUCTURAL GEOLOGY

www.elsevier.com/locate/jstrugeo

Up-dip partitioning of displacement components on the oblique-slip Clarence Fault, New Zealand

Andrew Nicol*, Russell Van Dissen

Institute of Geological & Nuclear Sciences Ltd, PO Box 30368, Lower Hutt, New Zealand

Received 29 November 2000; revised 25 September 2001; accepted 23 October 2001

Abstract

Active strike-slip faults in New Zealand occur within an obliquely-convergent plate boundary zone. Although the traces of these faults commonly delineate the base of mountain ranges, they do not always accommodate significant shortening at the free surface. Along the active trace of Clarence Fault in northeastern South Island, New Zealand, displaced landforms and slickenside striations indicate predominantly horizontal displacements at the ground surface, and a right-lateral slip rate of ca. 3.5–5 mm/year during the Holocene. The Inland Kaikoura mountain range occupies the hanging wall of the fault and rises steeply from the active trace to altitudes of ca. 3 km. The geomorphology of the range indicates active uplift and mountain building, which is interpreted to result, in part, from a vertical component of fault slip at depth. These data are consistent with the fault accommodating oblique-slip at depth aligned parallel to the plate-motion vector and compatible with regional geodetic data and earthquake focal-mechanisms. Oblique-slip on the Clarence Fault at depth is partitioned at the free surface into: (1) right-lateral displacement on the fault, and (2) hanging wall uplift produced by distributed displacement on small-scale faults parallel to the main fault. Decoupling of slip components reflects an up-dip transfer of fault throw to an off-fault zone of distributed uplift. Such zones are common in the hanging walls of thrusts and reverse faults, and support the idea that the dip of the oblique-slip Clarence Fault steepens towards the free surface.

Keywords: Transpression; Slip partitioning; Oblique-slip fault; New Zealand

1. Introduction

In continental crust undergoing transpression, fault-parallel and fault-normal components of oblique motion are commonly partitioned into spatially separate zones of strike-slip and dip-dip faulting (e.g. Fitch, 1972; Walcott, 1984; Oldow et al., 1990; Dewey and Lamb, 1992; McCaffrey, 1992). The development and degree of this classical form of strain partitioning has been attributed to a number of kinematic and mechanical factors, including: (1) obliquity between the convergence direction and fault strike (Braun and Beaumont, 1995; Teyssier et al., 1995), (2) non-parallelism of incremental and finite strain axes in the deforming crust (Tikoff and Teyssier, 1994), and (3) rheology of the crust (Platt, 1993). Several of these hypotheses have been tested in New Zealand where oblique right-lateral convergence occurs across the boundary between Pacific and Australian plates (e.g. Walcott, 1978, 1984, 1998; Bibby, 1981; DeMets et al., 1994). The central section of the Alpine Fault, New Zealand's best known interplate structure, accommodates oblique-slip, which is essentially parallel to the plate-motion vector (Sibson et al., 1979; Norris et al., 1990; Norris and Cooper, 1995), and the fault is regarded as being an example of non-partitioning of margin-parallel and -normal slip components in a transpressive orogen (e.g. Braun and Beaumont, 1995; Teyssier et al., 1995). North and south of the central section of the Alpine Fault the degree of slip partitioning increases with a greater component of the margin-normal slip apparently being transferred from the principal faults and into separate zones dominated by reverse faulting (Walcott, 1984; Cashman et al., 1992; Norris and Cooper, 2000). In these regions the principal faults appear to have accommodated mainly strike-slip displacements in the late Quaternary (e.g. Beanland, 1995; Little et al., 1998; Van Dissen and Nicol, 1999). Paradoxically, many of these strike-slip faults also mark the foot of mountain ranges with 1–3 km of relief (e.g. Fig. 1; see also Beanland, 1995; Little et al., 1998). The presence of these mountain ranges suggests that strike-slip faults at the free surface could be accommodating a vertical component of slip at depth and therefore change their slip direction relative to fault strike as they pass up through the crust.

* Corresponding author. Tel.: +64-4-5701444; fax: +64-4-5704600.
E-mail address: a.nicol@gns.cri.nz (A. Nicol).

0191-8141/02/$ - see front matter
PII: S0191-8141(01)00141-9

Fig. 1. Oblique aerial photograph looking northeast along the active trace of Clarence Fault (arrows) from 5 km north of its junction with Elliott Fault (Fig. 2). The fault dips steeply to the left of the photograph (NW) and coincides with the break in slope between the Inland Kaikoura Range and unfaulted piedmont surfaces in the valley floor downstream of the fault. The altitude difference between fault trace and range crest is ca. 1500–2000 m.

The Inland Kaikoura Range provides a spectacular example of a mountain range that rises sharply from the strike-slip Clarence Fault (Figs. 1 and 2). The altitude and steepness of the mountain range and its bold geomorphic expression argue against it being a relict feature inherited from a previous period of contraction. Based on summit-height accordances of assumed late Quaternary surfaces the range is inferred to be rapidly uplifting, perhaps at 5–10 mm/year (Wellman, 1979; Lamb and Bibby, 1989). Rapid uplift in the hanging wall of the fault suggests that this structure is not a simple strike-slip fault. Deep incision of drainages that flow from the range produce many exposures of the fault which, together with horizontal displacement measurements from the active trace and shortening data from regional geodetics and earthquake focal mechanisms, permit conclusions to be drawn about the kinematics of the fault. These data suggest that the Clarence Fault is oblique-slip at depth and at the ground surface is partitioned into right-lateral displacement and distributed off-fault uplift in the hanging wall. This model may apply to other strike-slip faults that coincide with mountain-range fronts.

2. Fault description and regional tectonics

The Clarence Fault is one of the principal elements of the Marlborough Fault System (comprising the Wairau, Awatere, Clarence and Hope Faults; see Fig. 2a), which links the Hikurangi subduction margin to the Alpine Fault (Fig. 2a and b) and accommodates $\geqq 75\%$ of plate boundary strain through northern South Island (Van Dissen and Yeats, 1991; Knuepfer, 1992; Holt and Haines, 1995). The fault can be regarded as comprising two parts, a western section that on average strikes 255°, approximately parallel to the plate-motion vector, and an eastern section that, on average, strikes about 25° anticlockwise to the plate-motion vector (Fig. 2). The eastern section of the fault has a prominent active trace, which bounds the southeastern foot of the Inland Kaikoura Range and is dominated by right-lateral displacements of, for example, relict streams, ridge crests and landslide margins (Van Dissen and Nicol, 1999). The Inland Kaikoura Range, located in the hanging wall of the Clarence Fault, rises abruptly from the fault trace (Fig. 1). To the northeast, the range is in the core of an anticline (Fig. 2) defined by warping of the contact between Cretaceous–Tertiary strata and Torlesse Supergroup basement (Lensen, 1962). These relationships suggest a close link between mountain building, folding of Cretaceous–Tertiary strata and uplift of the fault's hanging wall.

The active fault surface is well exposed in the steep walls of canyons incised into the range and typically separates Torlesse Supergroup basement of early Cretaceous age from Tertiary strata (Figs. 2 and 3). Within greywacke-dominated Torlesse basement rocks, bedding is typically deformed by tight to isoclinal folds, which are of pre-mid

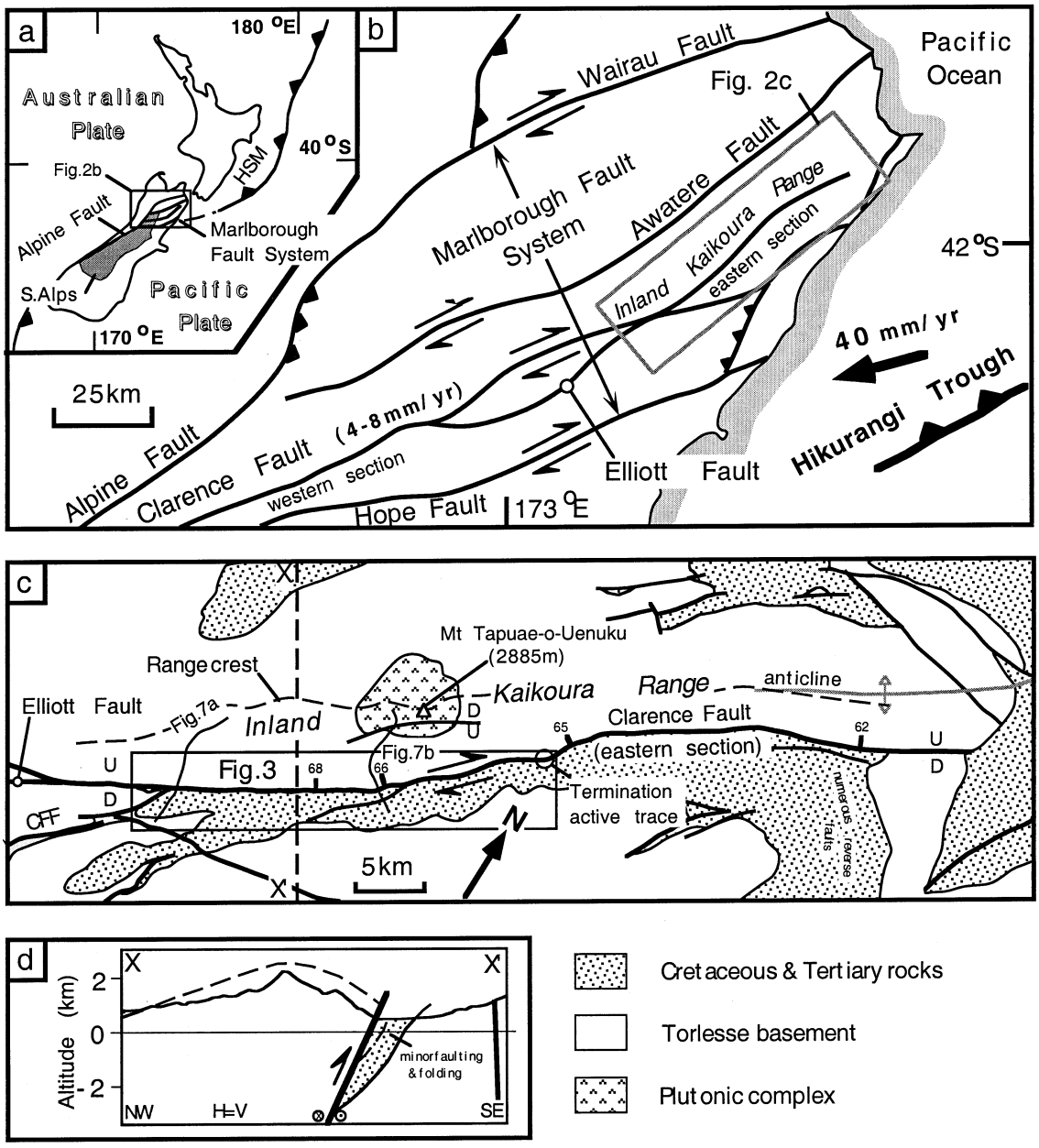

Fig. 2. (a) Plate-boundary setting of New Zealand. (b) Map of northeastern Marlborough, showing main active faults of the Marlborough Fault System (MFS), location of this study (i.e. the area covered by Fig. 2c) and plate-motion vector of 40 mm/year from DeMets et al. (1994). (c) Map and (d) cross-section of Clarence Fault and adjacent geology (Lensen, 1962; Prebble, 1976; Reay, 1993; Baker et al., 1994; Little and Jones, 1998; Van Dissen and Nicol, unpublished data 1997–1999). Tick marks and numbers show fault dip to the northwest. CFF is the Clock Face Fault and HSM the Hikurangi subduction margin.

Cretaceous age. Folding produced steeply dipping bedding of variable strike which, within 500 m of the fault, is sub-parallel to the Clarence Fault. In the footwall of the fault, Cretaceous–Tertiary volcanic and sedimentary rocks have moderate to steep dips on the limbs of upright folds that plunge gently to moderately, mostly to the northeast (Fig. 3). These folds typically have axial surfaces and hinges that are parallel to the active trace of Clarence Fault and may indicate shortening at a high angle to the fault. Within Torlesse basement rocks the Clarence Fault forms the south-eastern boundary of a 200–400-m-wide zone of intense brittle deformation (Fig. 4a and b). This zone was initially formed no later than a period of mafic-dike intrusion in the mid Cretaceous (ca. 100 Ma) and was reactivated during the late Cenozoic (Crampton et al., 1998). The active-slip surface of the Clarence Fault is typically marked by a <2-m-wide gouge zone which has a mean strike and dip of 048°/63°NW (Figs. 3 and 5). This strike is parallel to the range crest and ca. 25° anticlockwise to the Nuvel-1A relative plate-motion vector (DeMets et al., 1994; Figs. 2, 4 and 5).

The timing of initiation of late Cenozoic displacement on

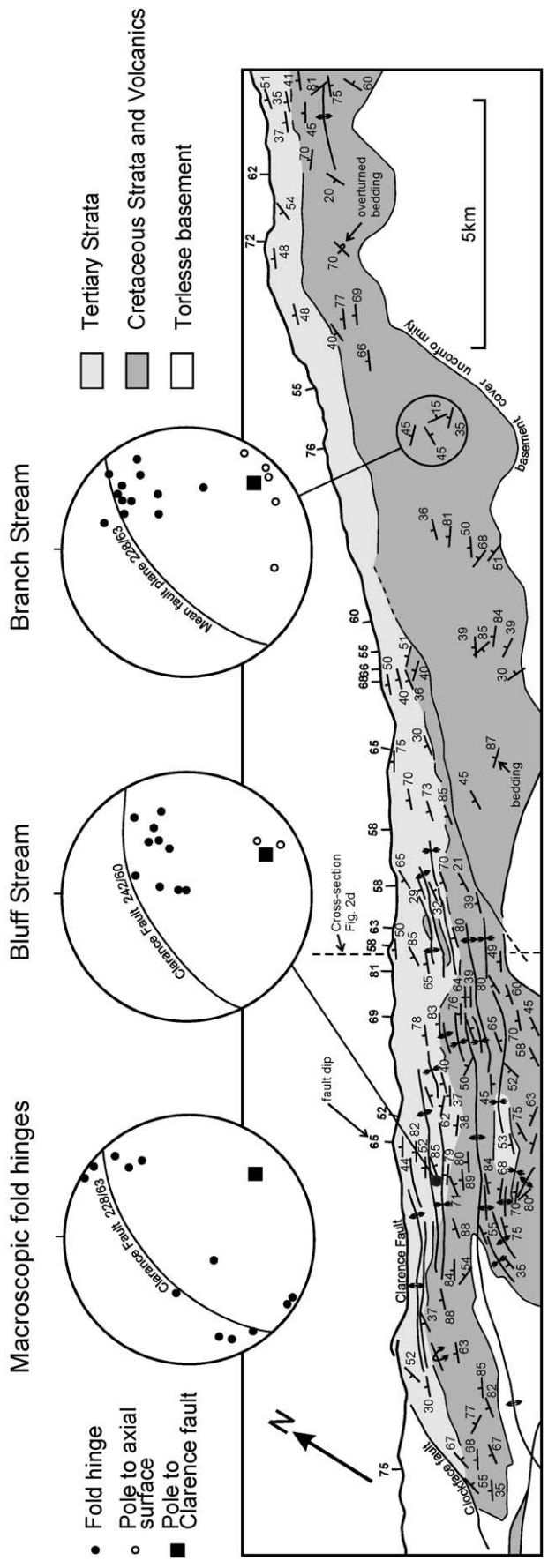

Fig. 3. Geological map of Clarence Fault and Cretaceous–Tertiary rocks in the footwall (see Fig. 2 for location). Data are from Reay (1993), Crampton and Isaac (unpublished data 1998) and this study. Stereograms (lower hemisphere) show geometric data for mesoscopic (Bluff and Branch streams) and macroscopic folds from the map area. Great circles denote mean attitude of Clarence Fault for each data set.

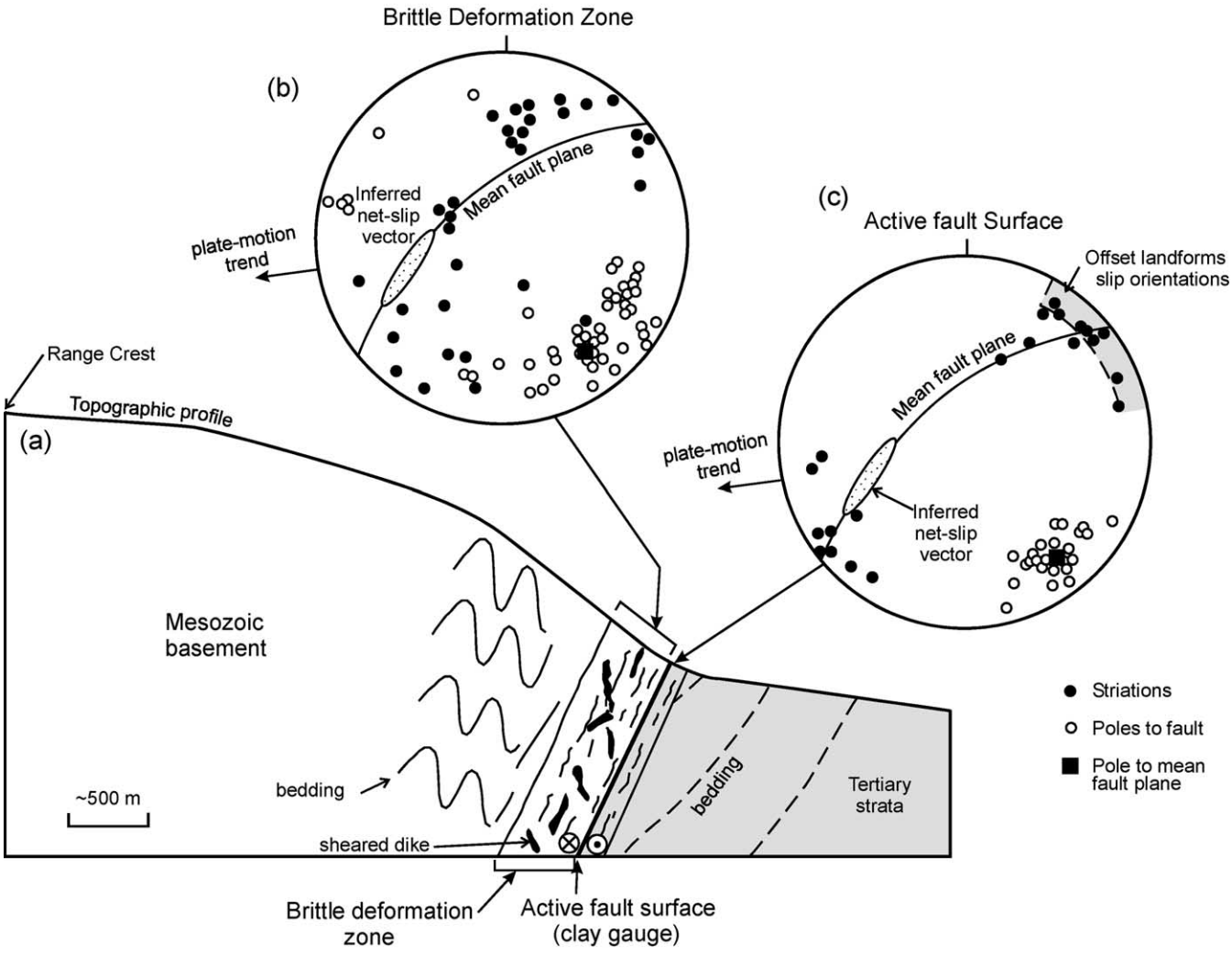

Fig. 4. (a) Schematic cross-section normal to the range and fault strike showing the Clarence Fault and its adjacent brittle-deformation zone. Stereograms (lower hemisphere) plot poles to, and slickenside striations on, (b) the faults in the adjacent brittle deformation zone and (c) the active fault surface. Orientation data were collected from fault exposures along a 50 km length of the fault. Orientation of plate-motion vector is from DeMets et al. (1994). Net-slip vector on Clarence Fault inferred from data in Section 3.2.

the Clarence Fault is uncertain. Angular and poorly sorted conglomerates along the Inland Kaikoura Range front together with fission track ages from the plutonic complex at the range crest suggest that a period of uplift and exhumation commenced at approximately 22 Ma. Baker and Seward (1996) calculate an average uplift rate of 0.2 mm/year since this time, over an order of magnitude less than the 5–10 mm/year proposed for the late Quaternary (Wellman, 1979; Lamb and Bibby, 1989), and suggest that the rate of uplift accelerated during the Quaternary.

Given present-day relative motion between the Pacific and Australian plates and the strike of the eastern section of the Clarence Fault, this part of the fault would be expected to be oblique-slip in a region undergoing no slip partitioning between structures, with reverse and right-lateral components of displacement. These expectations are consistent with focal mechanisms that range from strike-slip to thrust for earthquakes of magnitude 2.7–5.8 sampled to depths of ~20 km within the Australian plate in northeast Marlborough over a 30 year period (Arabasz and Robinson, 1976; Anderson et al., 1993; Reyners et al., 1997).

3. Fault displacements

Landforms displaced along the active trace (Fig. 6a) and slickenside striations from within the active fault zone (Fig. 4c) together with altitudes of topography and vertical separations of a top basement unconformity (Fig. 6b), provide estimates of the orientations and magnitudes of displacement vectors on the Clarence Fault.

3.1. Strike-slip on the active trace

The active trace accommodates mainly right-lateral displacements with ratios of horizontal slip (H) to vertical

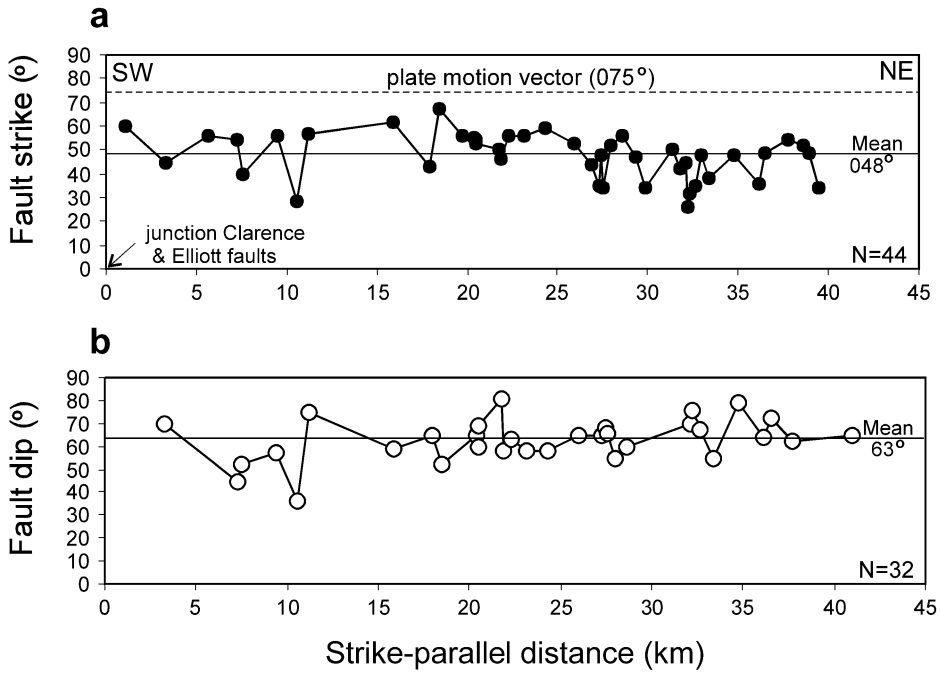

Fig. 5. Strike (a) and dip (b) attitudes for the active slip surface of Clarence Fault. Data were measured in outcrop or determined using structure contours on the fault surface, with each technique producing comparable results. Outcrop data were averaged from up to six measurements at each site.

slip (V) derived from tape measurements of displaced landforms of 10–15:1 (Reay, 1993; Van Dissen and Nicol, 1999). These ratios of H:V are consistent with slickenside striations from the active fault zone which plunge at mainly $<10°$ to the northeast (ca. 050°) and southwest (ca. 230°) (Fig. 4c).

Displaced Holocene landforms, including relict stream channels, gully walls, landslide margins, and ridge crests, trend approximately normal to the fault and record right-lateral displacements of 4–45 m on the active trace (Van Dissen and Nicol, 1999; Fig. 6a). The range of displacements is mainly due to the variable ages of the displaced landforms, with younger features recording displacements of about 7 and 14 m (Fig. 6a), which probably resulted from movement during the last one and two surface-rupturing earthquakes, respectively. Radiocarbon dates from displaced carbonaceous horizons in two stream-cut exposures of the fault constrain the timing of at least four paleoearthquakes and, together with displacement measurements, indicate right-lateral slip rates of ca. 3.5–5 mm/year over the last ca. 7 ka (Van Dissen and Nicol, 1999).

3.2. Throw and hanging wall off-fault uplift

The vertical component of Holocene displacement of landforms along the active trace is small (i.e. mainly <1–2 m) by comparison with the strike-slip displacement. These vertical displacements are normal in sense of dip-slip along the mapped length of the active trace (Fig. 2). A minor normal component of displacement on strike-slip fault traces is widely observed in New Zealand and may, in places, reflect near-surface dilation of fault-zone rocks (e.g. Wellman, 1996).

Juxtaposition of Torlesse basement against stratified Cretaceous–Tertiary rocks (Fig. 2) indicates a significant throw on the Clarence Fault since the mid-Cretaceous. Fig. 6b shows the projected altitude of the basement unconformity at the footwall cutoff and the range crest in the hanging wall, together with the altitudes of the range crest and the fault trace. Cretaceous–Tertiary rocks were deposited across the fault and, if the top of the basement had low relief prior to deposition of the overlying sediments (as appears to have been the case), then vertical offset of the basement unconformity provides an approximate measure of fault-related displacement. These data indicate a total vertical separation of ca. 4–8 km along much of the fault, consistent with fission-track dates from a plutonic complex (Fig. 2c), which are interpreted to indicate $\geqq$ 5–6 km net uplift in the hanging wall of the fault since about 22 Ma (Baker and Seward, 1996). At the ground surface, differential vertical displacement may have resulted from a combination of fault throw and off-fault hanging wall uplift (Fig. 2d). Based on the presence of coarse angular conglomerates next to the fault, it has been postulated that differential uplift across the Clarence Fault was initiated during a period of early Miocene contraction (Waters, 1988; Reay, 1993; Baker and Seward, 1996) and therefore the observed vertical separations are maxima for Quaternary deformation.

The occurrence of steep topography and deep drainage incision permits us to evaluate qualitatively the rates of late Quaternary erosion and uplift near the Clarence Fault, as others have done elsewhere (e.g. Keller, 1986; Merritts and

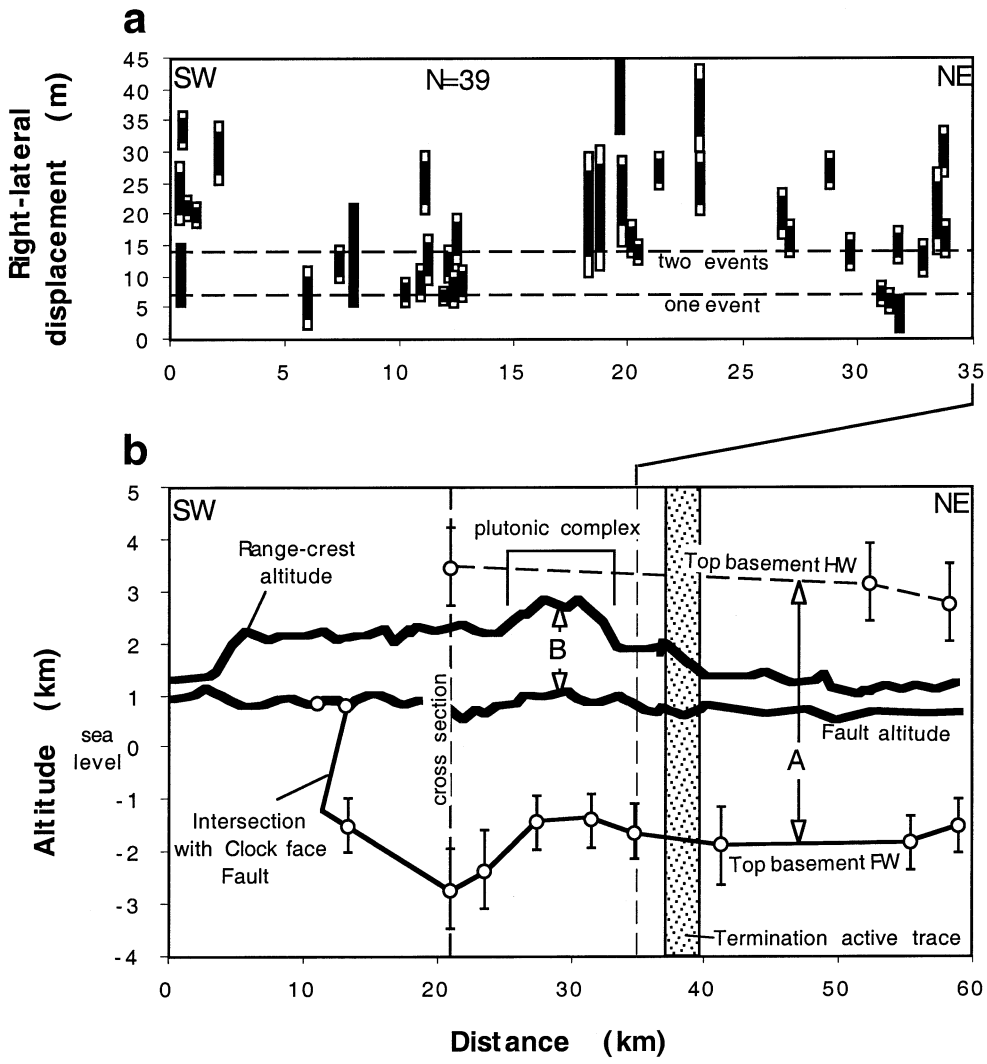

Fig. 6. Displacement data for Clarence Fault plotted against distance east of its junction with the Elliott Fault (see Fig. 2 for location). All data are projected onto a vertical plane parallel to the average fault strike (ca. 230°). (a) Right-lateral displacements measured from offset geomorphic markers trending at a high angle to the fault (e.g. relict gullies, ridges and landslide margins). Displacements were estimated to the $\pm 2\sigma$ (filled bars) $\pm 3\sigma$ (filled plus open bars) ranges. (b) Vertical-separation diagram showing the altitude of basement along the crest of the Inland Kaikoura Range and the fault trace together with the estimated altitude of the top basement unconformity at footwall (FW) cutoffs and the range crest in the hanging wall (HW) of the fault. Topography is from New Zealand 1:50,000 260 Topomap series which has a contour interval of 20 m. Altitudes of the Cretaceous–Tertiary basal unconformity were measured graphically from geological cross-sections (e.g. Fig. 2d) constructed normal to the fault using geological maps (Prebble, 1976; Reay, 1993; Van Dissen and Nicol, unpublished data 1997–1999). Error bars indicate uncertainties introduced by projecting the unconformity above and below the ground surface. (*A*) Indicates the estimated vertical separation for the basal unconformity (i.e. maximum vertical separation for the current deformation), while (*B*), the difference between the range crest and the fault may represent the minimum vertical separation for the Quaternary. See Section 3.2 for further discussion.

Vincent, 1989; Bürgmann et al., 1994). The Inland Kaikoura Range, located in the hanging wall of the Clarence Fault, rises up to ca. 2 km above the fault trace and contains the highest peak in New Zealand outside the Southern Alps (Mt Tapuae-o-Uenuku, 2885 m; Figs. 2 and 6). The highest parts of the range, including Mt Tapuae-o-Uenuku, consist of a plutonic complex and owe some of their altitude to the high erosional resistance of these crystalline rocks (Fig. 6b). The remainder of the range crest consists of Torlesse basement, which is dominated by greywacke and outcrops widely in New Zealand. Outside Marlborough, these rocks attain their highest altitude within the Southern Alps at Mt Cook (3754 m), the point where late Miocene to present day uplift is inferred to be greatest (e.g. Tippett and Kamp, 1993).

In cross-section, the Inland Kaikoura mountain range has an asymmetric morphology with steep southeast-facing slopes (typically 20–40°) between the range crest and fault (Figs. 1 and 7) and more gentle northwest-facing slopes (e.g. Fig. 2d). Steep southeast gradients are normal to the fault and typically decrease by a factor of 4–5 across the active trace (Figs. 1 and 7). Catchments that drain the steep southeast flank of the range typically trend normal to the crest and have deeply incised and V-shaped steep-walled canyons in the region upstream of the fault, while

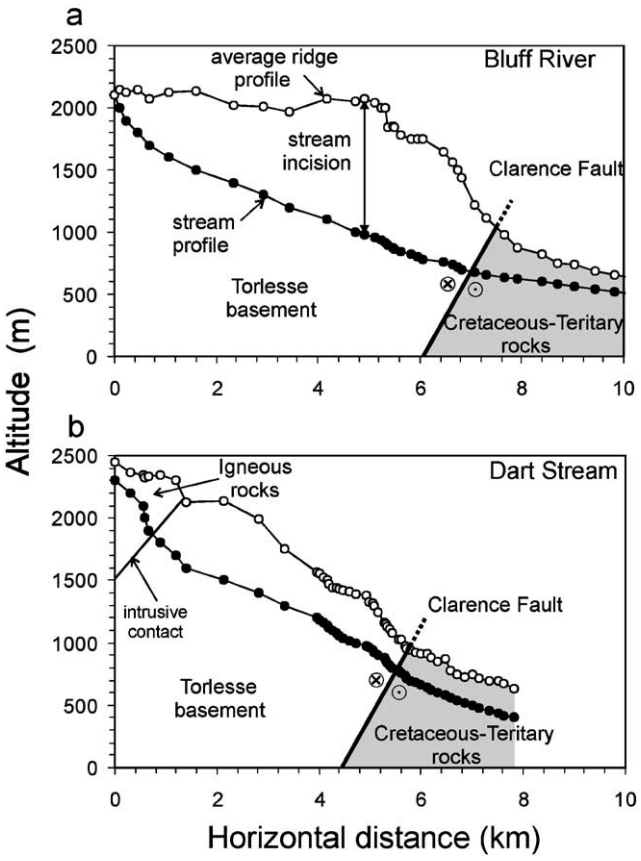

Fig. 7. Stream gradients and incision of: (a) Bluff River and (b) Dart Stream. These drainages originate within the range and flow southeastward across the Clarence Fault (see Fig. 2 for location). Incision is defined as the difference in altitude between the stream or riverbed and average ridge profile at the same point. Ridge profiles were produced by averaging the altitudes of ridges on each side of the drainage (see Bürgmann et al., 1994 for further details). Altitude data are from 20 m contours on 1:50,000 scale Topomap Awatere (infomap 260 O30). Differences in incision and streambed profiles between plots may, in part, result from the high erosional resistance of plutonic rocks.

downstream of the fault, streams are much less constricted and incised (Fig. 1). The profiles in Fig. 7 show some variability, but also share common elements, particularly where they cross the fault. Streams have concave-upwards profiles with bed gradients decreasing away from the range (Fig. 7). Superimposed on these broad concave upwards profiles, stream gradients are high upslope of the fault as compared with those in the footwall immediately below the fault, with a perceptible change in gradients at the fault (Fig. 7). Furthermore, the magnitude of stream incision typically decreases from 500–1000 m upstream of the active trace to <300 m downstream of the fault (Fig. 7). In summary, the high altitude of the range, together with the steep hillslopes and stream gradients and deep stream incision across the range, all suggest rapid rates of rock uplift in the hanging wall of the Clarence Fault during the late Quaternary. Alignment of the range parallel to the fault, coincidence of the foot of the range and the location of changes in stream gradients and incision with the fault trace (Fig.7), suggest that uplift of the mountain range was driven by movement on the fault.

Few data are available to constrain absolute uplift rates of the Inland Kaikoura Range or differential uplift rates between the range crest and Clarence Fault during the late Quaternary. A first order estimate of the rate of differential uplift across the Clarence Fault can be inferred using right-lateral slip rates of 4–8 mm/year from the western section of the fault, where it is essentially parallel to the plate-motion vector and accommodates pure strike-slip (Fig. 2b; calculated from data in Kieckhefer, 1979; Knuepfer, 1992). If net slip rates are conserved along the fault, then for right-lateral slip rates of 4–8 mm/year, an anticlockwise change in fault strike of about 25° and a decrease in fault dip from 90° to 63° from west to east, would produce rates of horizontal slip of ca. 2.5–5.0 mm/year and of vertical slip of ca. 3.0–5.5 mm/year on the fault at the ground surface adjacent to the Inland Kaikoura Range. These rates of vertical-slip are similar to the rate of differential uplift of 3–6 mm/year inferred from analysis of summit height accordances across the fault between the range crest and the Clarence River (see Fig. 8 for location; Lamb and Bibby, 1989). The predicted strike-slip rates are also comparable with those measured by Van Dissen and Nicol (1999) from offset of Holocene landforms. Comparison of the measured rate of strike-slip (ca. 3.5–5 mm/year) with the rate of vertical slip (ca. 3–5.5 mm/year) inferred above suggests an $H{:}V$ ratio of about 1:1, considerably less than the range of values observed from the active trace (i.e. 10–15:1).

Laterally extensive fluvial surfaces mainly restricted to the footwall of the Clarence Fault are unfaulted (e.g. Fig. 1), while there was no reverse displacement on the active trace of the Clarence Fault during the Holocene. Therefore, at the ground surface during this period of time, most of the proposed differential uplift was accommodated by deformation between the active trace and range crest, which is consistent with the asymmetry of the range, the steep rise of topography and the marked increase in stream gradients upstream of the fault. No significant faults (e.g. throw >500 m) synthetic to Clarence Fault have been identified between the range crest and fault, nor have any steps in the range front been recorded that might point to the presence of significant reverse faults. Instead, basement is deformed by numerous fractures and small-scale faults, which are mainly parallel to (e.g. see Fig.4b), and generally decrease in density with increasing distance from, the main fault. Slickenside and fibre striations on small-scale faults within a basement zone of brittle deformation up to 400 m from the active fault are typically more steeply plunging than those from the active fault surface, which are sub-horizontal (Fig. 4c). We have excluded faults from Fig. 4b that clearly predate Cretaceous mafic dikes, and the majority of the remaining slip data are slickenside striations and grooves on clay-rich fault surfaces. Such slip data have a low-preservation potential, as they are likely to be overprinted by subsequent slip events and probably record slip vectors

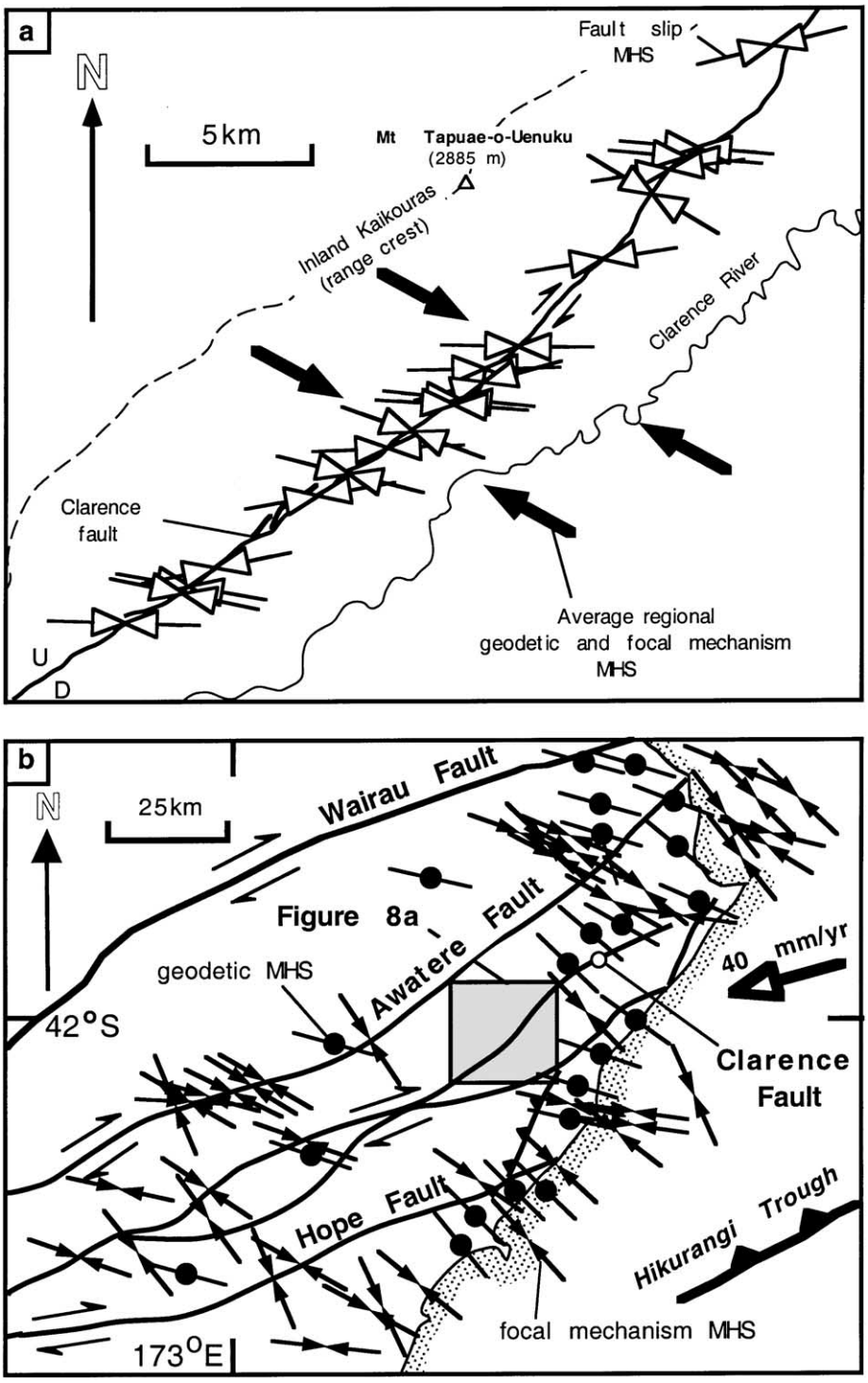

Fig. 8. (a) Local mean horizontal shortening (MHS) directions (open arrows) determined using a graphical technique (Marrett and Allmendinger, 1990) from slickenside striations within the active-fault zone and from offset landforms. Mean regional MHS in (a) from data in (b). MHS directions are parallel to the long axis of symbols. Area in (a) is located in (b). (b) Regional MHS directions derived from earthquake focal mechanisms (opposing arrows) (Arabasz and Robinson, 1976; Anderson et al., 1993; Reyners et al., 1997) and geodetic measurements (line and filled circle) (Bibby, 1976, 1981).

produced during the most recent phases of deformation. These data suggest that a greater component of throw is accommodated on small-scale faults in the immediate hanging wall of the active fault than occurs on the principal active slip surface, and support the view that off-fault differential uplift in basement rocks is accommodated by distributed slip on small-scale faults (see also Sylvester and Smith, 1976; Fig. 9, inset).

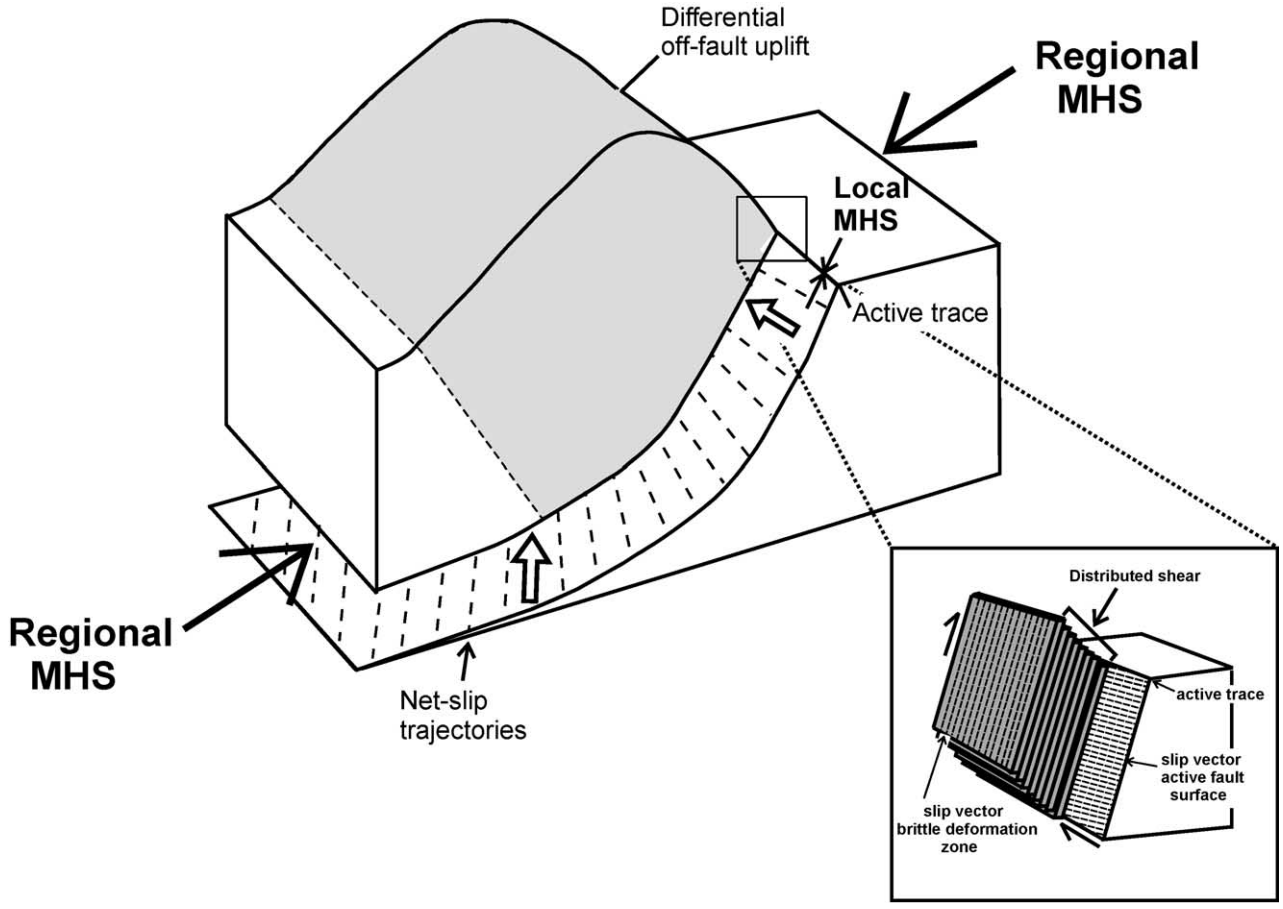

Fig. 9. Schematic diagram showing elements of the vertical-partitioning model for the eastern portion of Clarence Fault. Oblique-slip on the fault at depth is partitioned up-dip into right-lateral strike-slip on the fault and off-fault uplift at the ground surface. Dashed lines on the fault surface show the net motion of the fault hanging wall relative to a fixed footwall. Grey fill indicates the region of uplift in the hanging wall of the fault. Large arrows and MHS indicate the orientation of the maximum horizontal shortening on a regional scale and on the fault at depth, while small arrows and MHS on the active trace show the maximum horizontal shortening on the fault at the ground surface. See text for further discussion. Inset, schematic diagram showing partitioning of slip components at the ground surface into strike-slip on the main fault and dip-slip accommodated by distributed slip on fault surfaces parallel to, and in the hanging wall of, the principal fault. See Section 3.2 of text for further discussion.

4. Incremental horizontal shortening axes

Taken collectively, strike-slip displacements on the active trace and uplift of the mountain range in the hanging wall of the fault suggest that the fault is oblique-slip at depth, perhaps with slip parallel to the plate motion vector. Displacement data suggest a ~25° discrepancy between the orientation of slip on the Clarence Fault at the ground surface and the relative plate-motion vector (Fig. 4c). Classical slip partitioning between structures is absent in Marlborough (e.g. Little and Jones, 1998) and this discrepancy may reflect a change of the net-slip vector on the Clarence Fault in the middle to upper crust. If this interpretation is correct, then patterns of strain in the volume surrounding the Clarence Fault should be consistent with oblique-slip on the fault at depth rather than with strike-slip at the ground surface. In Fig. 8, we compare the orientations of maximum horizontal shortening (MHS) derived from slip directions on the active slip surface of the Clarence Fault (Fig. 8a) and from geodetic data and earthquake focal mechanisms for the wider region of the northeastern portion of the Marlborough Fault System (Fig. 8b). Fault slip is interpreted to accrue principally during large earthquakes (magnitudes 7–8), which ruptured the fault at the ground surface (Van Dissen and Nicol, 1999). Historic (i.e. last 30–100 years) geodetic and earthquake focal mechanism data characterise the patterns of strain that accumulated during the interseismic period between large-magnitude earthquakes on the principal faults of the Marlborough Fault System. Both data sets data record small increments of strain, which in geological terms are instantaneous and likely to be late Quaternary in age.

The direction of slip on the Clarence Fault is estimated from slickenside striations preserved on slip surfaces within clay gouge of the active fault surface where it is exposed in deeply incised streams (Fig. 4c). These data are used in conjunction with displaced landforms, which record the sense of slip, and with the graphical technique of Marrett and Allmendinger (1990) to derive the orientation of the principal strain axes. These strain axes are another

representation of the strike-slip displacement on the fault. They produce sub-horizontal (plunge <20°) maximum and minimum shortening axes and the intermediate axis is sub-vertical (plunge >70°). Fig. 8a shows the azimuth of maximum horizontal shortening (MHS) from 19 sites along the fault, with a 2-D vector mean trend of 092 ± 12° (standard error), i.e. on average 40° clockwise from the fault strike.

In Fig. 8 we compare the local azimuth of shortening on the Clarence Fault with regional MHS estimated using geodetic data and earthquake focal mechanisms. These geodetic and earthquake-derived MHS data (Fig. 8b) yield a 2-D vector mean azimuth of 121 ± 16° (standard error) and form part of a strain field which, on a regional scale, is generally uniform in azimuth across the plate boundary in South Island (e.g. Berryman, 1979; Pettinga and Wise, 1994; Little and Jones, 1998). Mean regional geodetic and earthquake-derived MHS trends on average at about 70° to the Clarence Fault and approximately 30° anticlockwise of the average MHS from fault-slip data (Fig. 8a). Local strain axes from the active fault at the free surface are therefore generally misaligned with regional strain data. Far-field MHS directions derived from geodetic and earthquake data are, however, consistent with net oblique-slip on the Clarence Fault. For example, the MHS derived by resolving the plate-motion vector onto the fault plane is 120 ± 10°. Thus, net oblique-slip on the Clarence Fault is compatible with both the orientations of bulk shortening and present-day relative plate motions, while MHS for strike-slip on the fault at the free surface is compatible with neither. These data are consistent with suggestions that the region enclosing the fault is experiencing transpression, that strike-slip is restricted to the fault in the upper crust and that the fault is oblique-slip at depth.

5. Partitioning of slip components

To account for the kinematics of the Clarence Fault, we must incorporate the following first-order observations: (1) mainly strike-slip along the active trace, (2) off-fault uplift and mountain building in the hanging wall of the fault, (3) no evidence of significant faults (e.g. >500 m throw) in the hanging wall or footwall of the fault that could accommodate contraction, (4) an average fault dip at the ground surface of 63°NW, and (5) a regional instantaneous maximum horizontal shortening direction that trends at about 70° to the fault.

To explain these observations, we propose that the Clarence Fault is oblique-slip at depth. The notion of oblique-slip on the fault is supported by the coincidence of an abrupt decrease of range altitude by 700–800 m (Fig. 6b) with the northeastern termination of the active trace in Clarence Valley (Fig. 2c), which suggests that uplift of the range and right-lateral displacements on the fault are related. We argue that oblique-slip on the fault at depth is partitioned into strike-slip on the fault and uplift off-fault approaching the free surface, with complete decoupling of slip components at the surface. Up-dip partitioning of slip components on a single structure is illustrated in Fig. 9 with, at the free surface, distributed dip-slip accommodated on small-scale reverse faults in the hanging wall of the principal strike-slip fault. This model requires that the vertical component of displacement on the fault attenuates more rapidly up-dip than the horizontal component. Variability in the rate of change of slip components may be attributed in part to changes in fault dip, as Jones and Wesnousky (1992) have argued for the San Andreas Fault. A concave-upwards curvature on the fault surface would be required to produce the apparent change in slip direction on the Clarence Fault (Fig. 9). These changes in slip direction occur because steeper parts of the fault surface are more optimally oriented to accommodate strike-slip, while dip-slip becomes increasingly difficult with higher dips as the component of shear stress across the fault surface decreases. Decreasing dip-slip with fault steepening has been proposed for compressional reactivation of listric faults (Sibson, 1995) and could lead to the antiformal buckles often observed in the hanging wall of concave-upwards faults (e.g. McClay, 1995).

Slip partitioning of the type in Fig. 9 requires a widening of the zone of deformation approaching the free surface. Up-dip increases in off-fault deformation and uplift may be enhanced by reduced overburden, which decreases the effective normal stress on existing small-scale faults and fractures. This process is influenced by redistribution of surface loads due to differential erosion and sedimentation (e.g. King et al., 1988) which, in areas of uplift and erosion, can produce effective tensile stresses and contribute to the formation of new fractures in rocks within 1–2 km of the free surface (e.g. Engelder, 1987). Small-scale faults and fractures reduce the bulk strength of rock and as a consequence the contrast in strength between the fault zone and the rock volume enclosing the fault may decrease approaching the ground surface. These changes in the rheology of rock close to the surface would tend to promote spatially distributed deformation, perhaps via movement on small-scale faults, at the expense of localisation of strain onto a single large fault and are consistent with Fig. 9 (inset).

Decreases in the magnitude of slip on steep strike-slip faults in basement can also occur approaching the free surface and typically produce en échelon folds, but require a ductile material or interlayered member to decouple deformation (see Sylvester, 1988). Folds adjacent to the active trace of Clarence Fault are in the main parallel to this structure (Fig. 3) and may have formed due to shortening at a high angle to the fault rather than bulk simple shear. Although transfer of strike-slip from the fault to en échelon folding is not supported by our data, slickenside striations on some small-scale faults do suggest a component of spatially distributed strike-slip in the hanging wall of the

fault (Fig. 4a). However, as our estimate of the strike-slip rate is consistent with that from the western section of the Clarence Fault (Section 3.2), this distributed strike-slip may be minor. Thus we do not see evidence for significant transfer of strike-slip on the Clarence Fault to distributed simple shear adjacent to the fault.

As the Clarence Fault is active, the question naturally arises as to how up-dip changes in the slip direction on a fault might be achieved during large magnitude earthquakes. One possibility is that up-dip partitioning of oblique-slip was accomplished by two types of 'characteristic' earthquake, one dominated by dip-slip that did not rupture the ground surface and produced differential uplift of the ground surface, and a second characterised by strike-slip, which formed the active trace. Alternatively, each earthquake could have had oblique-slip on the fault at depth with partitioning of horizontal and vertical components approaching the free surface. In either case the net-slip trajectory would be expected to rotate toward parallelism with fault-strike near the free surface resulting in a reduction in the magnitudes of the dip-slip component and net-slip vector upwards (Fig. 9); this may help to explain why oblique-slip faults are so rarely encountered at the surface. For the Clarence Fault the trend of the net-slip vector is postulated to rotate about 25° which, given the mean fault-plane orientation and a constant amount of strike-slip, could result in about a 20–40% decrease in the magnitude of net slip at the surface. In circumstances where up-dip changes in the net-slip direction are comparable with the orientations of earthquake slip, the slip/event, and thus magnitudes, could be underestimated, as is the case in regions of reverse faulting and related folding (e.g. Stein and King, 1984).

6. Discussion

A significant question remains regarding the general applicability of a model where the ratio of net dip-slip to strike-slip on a fault varies as it passes up through the crust. Within the Marlborough Fault System the eastern section of the Awatere Fault (see Fig. 2) is an example of a structure that is consistent with the model proposed. This fault is strike-slip at the free surface, approximately defines the southern boundary of a mountain range, and appears to be forming in association with off-fault uplift and deformation (Little et al., 1998; Benson, 2000; Benson et al., 2001). The slip direction of the Awatere Fault is not compatible with regional strain patterns (Little, 1995; Little and Jones, 1998) and the kinematics of Awatere Fault are consistent with oblique-slip on the fault at depth and strike-slip and off-fault uplift at the surface. Such a conclusion may also apply to numerous strike-slip faults that bound mountain fronts, including the eastern section of the Hope Fault and the Wairarapa Fault in New Zealand (Beanland, 1995), and perhaps also the San Andreas Fault adjacent to the San Gabriel and San Bernardino mountains (see Yeats et al., 1997).

In contrast to these faults, the central section of the Alpine Fault accommodates oblique-slip at the free surface, which is parallel to the plate convergence direction (Norris et al., 1990; Norris and Cooper, 1995, 2000). This section of the Alpine Fault is neither partitioned in the classical sense (Braun and Beaumont, 1995; Teyssier et al., 1995) nor does it appear to be characterised by up-dip decoupling of slip components in the manner suggested here. The angle between the plate convergence vector and fault strike is similar across both the Clarence (~25°) and Alpine (~29°) faults, and is unlikely to contribute to the observed differences in fault behaviour. There are, however, fundamental differences between the dips, rates of slip and net displacement on the two faults. Unlike the Clarence Fault, which dips steeply at the free surface (63°), the Alpine Fault dips moderately (~45–50°) to depths of 25 km (Davey et al., 1995). The shallower dip of the Alpine Fault would be expected to promote less transfer of dip-slip from the fault to the surrounding rock than occurs on the steeper Clarence Fault (see Section 5 for further discussion) and therefore the Alpine Fault is more likely to accommodate oblique-slip at the free surface. Disparities in the rheology of each fault zone relative to that of the surrounding crust and variations in the rates of exhumation between the two faults may also impact on fault-slip behaviour. For example, the high net displacement on the Alpine Fault and high exhumation rates of the Southern Alps (relative to those of the Clarence Fault and Inland Kaikoura Range) would tend to produce rheological strain softening and thermal weakening of the Alpine Fault (e.g. Batt and Braun, 1997; Koons et al., 1998; Ellis et al., 2001). These mechanisms are likely to promote a greater degree of oblique-slip localisation on the Alpine Fault than occurs on the Clarence Fault.

There are both similarities and differences between the up-dip changes in fault kinematics proposed here and classical partitioning of strike-slip and dip-slip onto separate and parallel structures. The kinematics of the Clarence Fault are comparable with that of palm tree structures (e.g. Lowell, 1972; Wilcox et al., 1973; Sylvester and Smith, 1976; Naylor et al., 1986) and of multiple slip-surface models (Abers and McCaffrey, 1988; Holdsworth and Strachan, 1991; Berberian et al., 1992; Bayasgalan et al., 1999), insofar as more steeply dipping parts of a fault, or system of faults, carry a greater component of strike-slip than shallower dipping parts of the fault(s). In detail, however, the Clarence Fault differs from these more widely recognised forms of strain partitioning in that it primarily reflects a change in kinematics along a single fault. Multiple-fault geometries, where strike-slip faults are vertical and located within the hanging wall of thrusts, are relatively easy to visualise using quasi-rigid block models. These multiple-fault models do not pose a kinematic problem with respect to the spatial distribution of uplift, as a thrust or reverse fault typically defines the range front

with strike-slip faults traversing topography of approximately constant altitude (i.e. within a mountain range or along a valley axis).

Multiple-fault geometries are kinematically similar to the single-fault model (Fig. 9) in that they both require a broadening of deformation approaching the free surface. Furthermore, high throw gradients on the principal fault (i.e. the fault that carries strike-slip at the surface) are implicit in both models and form in association with transfer of contraction from the principal fault to footwall thrusting or to off-fault uplift in the hanging wall, respectively. The transfer of contraction between structures or from discontinuous (i.e. faulting) to continuous (e.g. expressed as folding in layered sequences) styles of deformation is widely observed for contractional structures in, for example, the Canadian Rockies and South Wales (UK) (e.g. Dahlstrom, 1970; Ellis and Dunlap, 1988; Nicol et al., 2002), and need not negate either model.

The proposed geometric simplicity of slip on the Clarence Fault in contrast to multiple-fault partitioning models, may be influenced by two factors. First, the Clarence Fault is a reactivated structure, which experienced extension during the mid-Cretaceous (Reay, 1993; Crampton et al., 1998) and probably inherited its geometry from a pre-existing normal fault. Second, sub-horizontal layering above, or in the footwall of, an oblique- or strike-slip fault experiencing a component of contraction may promote thrusting on layer-parallel slip surfaces near to the surface (e.g. Sylvester, 1988; Bayasgalan et al., 1999). Sub-horizontal layering is not present adjacent to the Clarence Fault near to the free surface, probably because high rates of erosion have resulted in removal of all mid-Miocene and younger strata. As a consequence there is no prospect of near-surface thrusting associated with delamination of a sub-horizontal sequence.

In regions of transpression classical strain partitioning of slip components onto separate and parallel structures (e.g. Fitch, 1972; Walcott, 1984; Oldow et al., 1990; McCaffrey, 1992), and non-partitioned oblique-slip faults (e.g. Alpine Fault; Norris and Cooper, 2000) define a range of possible fault kinematics. We argue that this range should be broadened to include those faults that exhibit up-dip changes in slip components on individual structures, as proposed here. These three different types of fault behaviour may represent end-members in a continuum. A number of factors have been proposed to account for the development of classical strain partitioning including obliquity between the convergence direction and fault strike and rheology of the crust (see Section 1 and references therein). By comparison factors influencing up-dip partitioning of slip components on a single structure are much less well known and may include fault dip, crustal rheologies and rates of deformation. Whatever the precise mechanisms involved, in regions exhibiting classical strain partitioning, faults which are strike-slip at the ground surface may accommodate a component of dip-slip at depth. This could be the case for some faults in the Hikurangi subduction margin, North Island, New Zealand, which is experiencing transpression and has been postulated to be completely partitioned (Walcott, 1984; Cashman et al., 1992; Beanland, 1995). In this region the strike-slip Wairarapa Fault, for example, defines the eastern margin of the Axial Ranges and may accommodate a component of dip-slip at depth, as appears to have been the case during the 1855 Wairarapa earthquake (Darby and Beanland, 1992).

7. Conclusions

Kinematic data from the Clarence Fault, New Zealand, indicate that transpression across the fault is associated with horizontal displacements on the active trace and distributed uplift in its hanging wall producing a mountain range. To reconcile these observations we propose net oblique-slip on the fault at depth approximately parallel to the plate-motion vector and compatible with the regional trend of the maximum horizontal shortening. Oblique-slip on the fault at depth is partitioned at the surface into right-lateral displacement on the fault and hanging wall uplift associated with distributed slip on small-scale faults parallel to the Clarence Fault. Decoupling of slip components reflects an up-dip transfer of the vertical displacement on the fault to off-fault uplift, as is widely described for thrusts and reverse faults, and is consistent with an upward steepening of the fault.

Acknowledgements

Funding for this work was provided by the New Zealand Foundation for Research, Science and Technology. Kelvin Berryman, Des Darby, Susan Ellis, Tim Little, Richard Norris, Arthur Sylvester, Basil Tikoff and Bob Yeats are thanked for their thorough and constructive reviews of earlier versions of the manuscript. Discussions with Kelvin Berryman, Hugh Bibby, Des Darby, Susan Ellis, Don Garlic, Tim Little, David Rhoades and Bob Yeats proved useful. Institute of Geological & Nuclear Sciences contribution number 2261.

References

Abers, G.A., McCaffrey, R., 1988. Active deformation in the New Guinea fold-and-thrust belt: seismological evidence for strike-slip faulting and basement-involved thrusting. Journal of Geophysical Research 93, 13332–13345.

Anderson, H., Webb, T., Jackson, J.A., 1993. Focal mechanisms of large earthquakes in the South Island of New Zealand: implications for the accommodation of Pacific–Australia plate motion. Geophysical Journal International 115, 1032–1054.

Arabasz, W.J., Robinson, R., 1976. Microseismicity and geological structure in the northern South Island, New Zealand. New Zealand Journal of Geology and Geophysics 19, 569–601.

Baker, J., Seward, D., 1996. Timing of Cretaceous extension and Miocene

compression in northeastern South Island: constraints from Rb–Sr and fission track dating of an igneous pluton. Tectonics 15, 976–983.

Baker, J., Gamble, J.A., Graham, I.G., 1994. Geology of the Tapuaenuku Igneous complex, Marlborough, New Zealand. New Zealand Journal of Geology and Geophysics 37, 249–268.

Batt, G., Braun, J., 1997. On the thermo-mechanical evolution of compressional orogens. Geophysical Journal International 128, 364–382.

Bayasgalan, A., Jackson, J., Ritz, J.-F., Carretier, S., 1999. 'Forebergs', flower structures, and the development of large intra-continental strike-slip faults: Gurvan Bogd fault system in Mongolia. Journal of Structural Geology 21, 1285–1302.

Beanland, S., 1995. The North Island dextral fault belt. Unpublished PhD, Victoria University of Wellington, Wellington, New Zealand.

Benson, A., 2000. Late Quaternary deformation and paleoseismicity of the Awatere Fault, South Island, New Zealand. Unpublished MSc, Victoria University of Wellington, Wellington, New Zealand.

Benson, A., Hill, N., Little, T.A., Van Dissen, R.J., 2001. Paleoseismicity, rates of active deformation, and structure of the Lake Jasper pull-apart basin, Awatere fault, New Zealand. Victoria University of Wellington School of Earth Sciences Consulting Report No. 2001/1 (EQC Research Report 97/262).

Berberian, M., Qorashi, M., Jackson, J.A., Preistley, K., Wallace, T., 1992. The Rudbar–Tarom earthquake of 20 June 1990 in NW Persia: preliminary field and seismological observations, and its tectonic significance. Bulletin Seismological Society America 82, 1726–1755.

Berryman, K., 1979. Active faulting and derived PHS directions in the South Island, New Zealand. Royal Society of New Zealand Bulletin 18, 29–34.

Bibby, H.M., 1976. Crustal strain across the Marlborough Faults, New Zealand. New Zealand Journal of Geology and Geophysics 19, 407–475.

Bibby, H.M., 1981. Geodetically determined strain across the southern end of the Tonga–Kermadec–Hikurangi subduction system. Geophysical Journal of the Royal Astronomical Society 66, 513–533.

Braun, J., Beaumount, C., 1995. Three-dimensional numerical experiments of strain partitioning at oblique plate boundaries: implications for contrasting tectonic styles in the southern Coast Ranges, California, and central South Island, New Zealand. Journal of Geophysical Research 100, 18059–18074.

Bürgmann, R., Arrowsmith, R., Dumitru, T., McLaughlin, R., 1994. Rise and fall of the southern Santa Cruz Mountains, California, from fission track, geomorphology, and geodesy. Journal of Geophysical Research 99, 20181–20202.

Cashman, S.M., Kelsey, H.M., Erdman, C.F., Cutten, H.N.C., Berryman, K.R., 1992. Strain partitioning between structural domains in the forearc of the Hikurangi subduction zone, New Zealand. Tectonics 11, 242–257.

Crampton, J.C., Laird, M.G., Nicol, A., Hollis, C., Van Dissen, R., 1998. Geology at the northern end of the Clarence Valley, Marlborough: a complete record spanning the Rangitata to Kaikoura orogenies. Geological Society of New Zealand, Miscellaneous Ppublication 101B.

Dahlstrom, C.D.A., 1970. Structural geology in the eastern margin of the Canadian Rocky Mountains. Bulletin of Canadian Petroleum Geology 18, 332–406.

Darby, D., Beanland, S., 1992. Possible source models for the 1855 Wairarapa earthquake, New Zealand. Journal of Geophysical Research 97 (B9), 12375–12389.

Davey, F.J., Henyey, T., Kleffmann, S., Melhuish, A., Okaya, D., Stern, T.A., Woodward, D.J., 1995. Crustal reflections from the Alpine Fault zone, South Island, New Zealand. New Zealand Journal of Geology and Geophysics 38, 601–604.

DeMets, C., Gordon, R.G., Argus, D.F., Stein, S., 1994. Effect of recent revisions to the geomagnetic reversal time scale on estimates of current plate motions. Geophysical Research Letters 21, 2191–2194.

Dewey, J.F., Lamb, S.H., 1992. Active tectonics of the Andes. Tectonophysics 205, 79–95.

Ellis, M.A., Dunlap, W.J., 1988. Displacement variation along thrust faults: implications for the development of large faults. Journal of Structural Geology 10, 183–192.

Ellis, S., Wissing, S., Pfiffner, A., 2001. Strain localisation as a key to reconciling experimentally derived flow-law data with dynamic models of continental collision. International Journal of Earth Sciences 90, 168–180.

Engelder, T., 1987. Joint and shear fractures in rock. In: Atkinson, B.K. (Ed.). Fracture Mechanics of Rock. Academic Press, Orlando, pp. 27–69.

Fitch, T.J., 1972. Plate convergence, transcurrent faults, and internal deformation adjacent to southeast Asia and the western Pacific. Journal of Geophysical Research 77, 4432–4460.

Holdsworth, R.E., Strachan, R.A., 1991. Interlinked system of ductile strike-slip and thrusting formed by Caledonian sinistral transpression in northeastern Greenland. Geology 19, 510–513.

Holt, W.E., Haines, A.J., 1995. The kinematics of northern South Island, New Zealand, determined from geologic strain rates. Journal of Geophysical Research 100, 17991–18010.

Jones, C.H., Wesnousky, S.G., 1992. Variations in strength and slip rate along the San Andreas Fault System. Science 256, 83–86.

Keller, E.A., 1986. Investigation of active tectonics: use of surficial earth processes. In: Wallace, R.E. (Ed.). Active Tectonics: Studies in Geophysics Series, Geophysics Research Forum. National Academy Press, Washington, DC, pp. 136–147.

Kieckhefer, R.M., 1979. Sheets M31D, M31A, N31C and pts M32A & M32B, Leader Dale (1st Edition); Sheets N31B & N31D, Dillon (1st Edition); Sheets O30C & O31A, Lake McRae (1st Edition), Late Quaternary Tectonic Map of New Zealand 1:50,000. 3 maps and text. Department of Scientific and Industrial Research, Wellington.

King, G.C.P., Stein, R.S., Rundle, J.B., 1988. The growth of geological structures by repeated earthquakes. Journal of Geophysical Research 93, 13307–13318.

Knuepfer, P.L.K., 1992. Temporal variations in latest Quaternary slip across the Australian–Pacific plate boundary, northeastern South Island, New Zealand. Tectonics 11, 449–464.

Koons, P.O., Norris, R.J., Cooper, A.F., Craw, D., 1998. Mechanics of a single structure accommodating oblique convergence: the development of the Alpine Fault. Geological Society of New Zealand Miscellaneous Publication 101A, 138.

Lamb, S.H., Bibby, H.M., 1989. The last 25 Ma of rotational deformation in part of the New Zealand plate boundary zone. Journal of Structural Geology 11, 473–492.

Lensen, G.J., 1962. Sheet 16—Kaikoura. Geological map of New Zealand 1:250,000. Department of Scientific and Industrial Research, Wellington.

Little, T.A., 1995. Brittle deformation adjacent to the Awatere strike-slip fault in New Zealand: fault patterns, scaling relationships, and displacement partitioning. Geological Society of America Bulletin 107, 1255–1271.

Little, T.A., Jones, A., 1998. Seven million years of strike-slip and related off-fault deformation, northeastern Malborough fault system, South Island, New Zealand. Tectonics 17, 285–302.

Little, T.A., Grapes, R., Berger, G.W., 1998. Late Quaternary strike-slip on the eastern part of the Awatere fault, South Island, New Zealand. Geological Society of America Bulletin 110, 127–148.

Lowell, J.D., 1972. Spitsbergen Tertiary orogenic belt and the Spitsbergen fracture zone. Geological Society of America Bulletin 83, 3091–3102.

Marrett, R., Allmendinger, R.W., 1990. Kinematic analysis of fault-slip data. Journal of Structural Geology 12, 973–986.

McCaffrey, R., 1992. Oblique convergence, slip vectors, and forearc deformation. Journal of Geophysical Research 97, 8905–8915.

McClay, K.R., 1995. The geometries and kinematics of inverted fault systems: a review of analogue model studies. In: Buchanan, J.G., Buchanan, P.G. (Eds.), Basin Inversion. Geological Society of London Special Publication 88, pp. 97–118.

Merritts, D., Vincent, K.R., 1989. Geomorphic response of coastal streams to low, intermediate, and high rates of uplift, Mendocino triple junction

region, northern California. Geological Society of America Bulletin 101, 1373–1388.

Naylor, M.A., Mandl, G., Sijpesteijn, C.H.K., 1986. Fault geometries in basement-induced wrench faulting under different initial stress states. Journal of Structural Geology 8, 737–752.

Nicol, A., Gillespie, P.A., Walsh, J.J., Childs, C., 2002. Thrust relays and associated folding in layered sequences. Journal of Structural Geology in press.

Norris, R.J., Cooper, A.F., 1995. Origin of small-scale segmentation and transpressional thrusting along the Alpine fault, New Zealand. Geological Society of America Bulletin 107, 231–240.

Norris, R.J., Cooper, A.F., 2000. Late Quaternary slip rates and slip partitioning on the Alpine Fault, New Zealand. Journal of Structural Geology 23, 507–520.

Norris, R.J., Koons, P.O., Cooper, A.F., 1990. The obliquely-convergent plate boundary in the South Island of New Zealand: implications for ancient collision zones. Journal of Structural Geology 12, 715–725.

Oldow, J.S., Bally, A.W., Ave Lallement, H.G., 1990. Transpression, orogenic float, and lithospheric balance. Geology 18, 991–994.

Pettinga, J.R., Wise, D.U., 1994. Paleostress adjacent to the Alpine fault: Broader implications from fault analysis near Nelson, South Island, New Zealand. Journal of Geophysical Research 99, 2727–2736.

Platt, J.P., 1993. Mechanics of oblique convergence. Journal of Geophysical Research 98, 16239–16256.

Prebble, W.M., 1976. The geology of the Kekerengu–Waima River district, north east Marlborough. M.Sc. thesis, Victoria University of Wellington.

Reay, M.B., 1993. Geology of the Middle Clarence Valley. Institute of Geological & Nuclear Sciences geological map 10, scale 1:50,000. Institute of Geological & Nuclear Sciences Ltd, Lower Hutt, New Zealand.

Reyners, M., Robinson, R., McGinty, P., 1997. Plate coupling in the northern South Island and southernmost North Island, New Zealand, as illuminated by earthquake focal mechanisms. Journal of Geophysical Research 102, 8331–8363.

Sibson, R.H., 1995. Selective fault reactivation during basin inversion: potential for fluid redistribution through fault-valve action. In: Buchanan, J.G., Buchanan, P.G. (Eds.), Basin Inversion, Geological Society of London Special Publication 88, pp. 3–19.

Sibson, R.H., White, S.H., Atkinson, B.K., 1979. Fault rock distribution and structure within the Alpine Fault Zone: a preliminary account. In: Walcott, R.I., Cresswell, M.M. (Eds.), The Origin of the Southern Alps. Royal Society of New Zealand Bulletin 18, pp. 55–65.

Stein, R.S., King, G.C.P., 1984. Seismic potential revealed by surface folding: 1983 Coalinga, California, Earthquake. Science 224, 869–872.

Sylvester, A.G., 1988. Strike-slip faults. Geological Society of America Bulletin 100, 1666–1703.

Sylvester, A.G., Smith, R.R., 1976. Tectonic transpression and basement-controlled deformation in the San Andreas fault zone, Salton Trough, California. American Association of Petroleum Geologists Bulletin 60, 2081–2102.

Teyssier, C., Tikoff, B., Markley, M., 1995. Oblique plate motion and continental tectonics. Geology 23, 447–450.

Tikoff, B., Teyssier, C., 1994. Strain modeling of displacement-field partitioning in transpressional orogens. Journal of Structural Geology 16, 1575–1588.

Tippett, J.M., Kamp, P.J.J., 1993. Fission track analysis of the Late Cenozoic vertical kinematics of continental Pacific crust, South Island, New Zealand. Journal of Geophysical Research 98, 16119–16148.

Van Dissen, R., Yeats, R.S., 1991. Hope fault, Jordan thrust, and uplift of the seaward Kaikoura Range, New Zealand. Geology 19, 393–396.

Van Dissen, R., Nicol, A., 1999. Paleoseismicity of the middle Clarence Valley section of the Clarence Fault, Marlborough, New Zealand. Geological Society of New Zealand, Miscellaneous Publication 107A.

Walcott, R.I., 1978. Present tectonics and late Cenozoic evolution of New Zealand. Geophysical Journal of the Royal Astronomical Society 52, 137–164.

Walcott, R.I., 1984. Reconstructions of the New Zealand region for the Neogene. Palaeogeography, Palaeoclimatology, Palaeoecology 46, 217–231.

Walcott, R.I., 1998. Modes of oblique compression: late Cenozoic tectonics of the South Island, New Zealand. Reviews of Geophysics 36, 1–26.

Waters, D.A., 1988. The Flags Creek Thrust, Marlborough, New Zealand. B.Sc. Hons thesis, Victoria University of Wellington.

Wellman, H.W., 1979. An uplift map for the South Island of New Zealand, and a model for the uplift of the Southern Alps. In: Walcott, R.I., Cresswell, M.M. (Eds.), The Origin of the Southern Alps. Royal Society of New Zealand Bulletin 18, pp. 13–20.

Wellman, H.W., 1996. Earthquake rents: throw reversal of compaction–decompaction. Geological Society of New Zealand Newsletter 110, 49–50.

Wilcox, R.E., Harding, T.P., Seely, D.R., 1973. Basic wrench tectonics. American Association of Petroleum Geologists Bulletin 57, 74–96.

Yeats, R.S., Sieh, K., Allen, C., 1997. The Geology of Earthquakes. Oxford University Press.